International Journal of Thermophysics, Vol. 20, No. 4, 1999

Scanning the Melting Curve of Tungsten by a Submicrosecond Wire-Explosion Experiment[1]

A. Kloss,[2] H. Hess,[2,3] H. Schneidenbach,[2] and R. Grossjohann[2]

Measurements of temperature and density during a wire-explosion experiment at atmospheric pressure are described. The measurements encompass a parameter range from the solid to near the critical point. The influence of a polytetrafluoroethylene coating of the wire, necessary to prevent surface discharges, on the temperature and density measurements is investigated. The melting curve of tungsten up to 4000 K is detemined.

KEY WORDS: heat of fusion; high temperatures; measurement of density; measurement of temperature; melting; melting curve; refractory metals; tungsten; wire explosion.

1. INTRODUCTION

Wire-explosion experiments are well established for the investigation of thermophysical properties of metals, e.g., specific heat, heat of fusion, thermal expansion, etc. Usually, these experiments are carried out in high-pressure cells [1–3] or in capillaries [4, 5]. The melting of the sample is reached, typically, within some microseconds.

In the first group of experiments, isobaric conditions are assumed at pressures up to 0.8 GPa. These experiments do not reach the critical pressure of refractory metals, e.g., about 1.6 GPa for tungsten [6]. Optically measured properties of the sample, i.e., temperature and geometrical dimensions, are difficult to determine with small errors, due to the strong

[1] Paper presented at the Fifth International Workshop on Subsecond Thermophysics, June 16–19, 1998, Aix-en-Provence, France.

[2] Institute of Low-Temperature Plasma Physics, F.-L.-Jahn-Str. 19, D-17489 Greifswald, Germany.

[3] To whom correspondence should be addressed.

0195-928X/99/0700-1199$16.00/0

changes in the refractive index of the surrounding substance and its relatively high specific heat and thermal conductivity.

In the second group of experiments, homogeneous conditions are assumed after the capillary is completely filled with the expanding metal. In this case the measurements start at a density considerably lower than the solid density. Optical measurements are even more difficult than in the first group.

If values such as expansion and temperature are to be measured, the exploding wire should be "as pure as possible." With this condition, i.e., without a serious capsulation, the required high-pressure has to be reached due to the own inertia of the sample. Therefore, a wire-explosion experiment was set up to reach melting after 100 to 200 ns [7, 8].

2. EXPERIMENTAL SET-UP

The experimental arrangement shown in Fig. 1 is described in detail in Refs. 7 and 8. In a low-inductive ($L_C = 60$ nH) and low-resistive ($R_C = 29$ mΩ) circuit, a capacitor ($C_L = 329$ nF) is discharged into a wire-shaped sample. The present experiments were carried out with tungsten wires (length, 5.0 mm; diameter, 200 μm) without and with a coating of polytetrafluorethylene (PTFE) with a thickness of 50 μm [9].

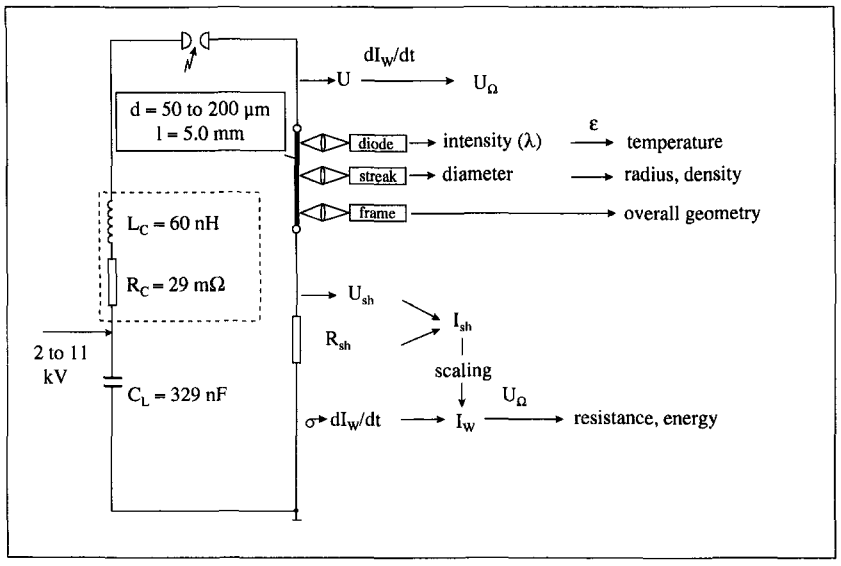

Fig. 1. Schematic of the experimental arrangement.

The capacitor was charged over the range of 7.5 to 14 kV. This leads to maximum rates of energy dissipation of 1.5 to 5.5×10^{12} $W \cdot mol^{-1}$, a value that is used to characterize a single shot, and heating rates of 1.8 to 9.6×10^{10} $K \cdot s^{-1}$.

The time derivative of the current through the wire (dI_W/dt) is measured by a Rogowski coil, numerically integrated and scaled with the current I_{sh} that is measured with the help of a shunt resistor R_{sh}. The voltage U is measured with a compensated and low-inductive voltage divider. The ohmic voltage U_Ω is obtained after having substracted the remaining inductive part of voltage. The resistance of the wire and the energy dissipated in the entire material are calculated from the voltage U_Ω and the current I_W.

The radiation from the surface is observed with a Si–Pin photodiode (Tektronix P6711A). A streak camera (Hadland; Imacon 500) records the radial development of one cross section of the wire. The overall geometry and the occurrence of surface discharges are observed with a framing camera (Hadland; Imacon 468), which takes four images, each with an exposure time of 10 ns.

3. MEASUREMENT OF TEMPERATURE

The temperature of the exploding wire will reach more than 10,000 K and is measured pyrometrically. Therefore, a spot with a diameter of 23 μm is focused on the entrance of a fiber, which will guide the radiation to the photodiode. The electrical signal from the diode is split and measured in parallel with two channels of the oscilloscope. The sensitivity of one channel is set to fit the entire signal. The other channel has a resolution that is 10 times higher, to resolve better the signal corresponding to the melting plateau. With this method, an effective resolution of one part in a thousand is achieved. The overdrive of the second channel has no further negative effect.

The surface temperature can be calculated from the radiation by Planck's law,

$$S_\lambda = \iiint \varepsilon(\lambda, T)\, \zeta(\lambda)\, 2 \frac{hc_0^2}{\lambda^5} \frac{1}{e^{hc_0/\lambda kT} - 1}\, d\Theta\, dF\, d\lambda \tag{1}$$

where S_λ is the spectral intensity at the wavelength λ, $\varepsilon(\lambda, T)$ is the emissivity, $\zeta(\lambda)$ is the transmittance of all optical components, dF is the observed area, $d\Theta$ is the angle of observation, $d\lambda$ is the spectral bandwidth, c_0 is the speed of light, h is Planck's constant, and k is Boltzmann's constant.

If for one wavelength λ, the intensity $S_{\lambda,\mathrm{m}}$ is known for a given temperature T_m, it is possible to calculate the temperature from the ratio between S_λ and $S_{\lambda,\mathrm{m}}$:

$$T = \frac{\mathrm{const}_1}{\ln\left(\mathrm{const}_2 \dfrac{\varepsilon(\lambda, T)}{\varepsilon(\lambda, T_\mathrm{m})} \dfrac{S_{\lambda,\mathrm{m}}}{S_\lambda}\right) - 1} \tag{2}$$

with $\mathrm{const}_1 = hc_0/\lambda k$ and $\mathrm{const}_2 = e^{hc_0/\lambda k T_\mathrm{m}} - 1$.

For this self-calibration method, the intensity must be measured at one wavelength λ with a small bandwidth $d\lambda$, the geometry of the pyrometer has to be maintained and the emissivity $\varepsilon(\lambda, T)$ must be known.

The actual measurements were carried out at 650 ± 40 nm. This is far from the intense spectral lines of tungsten [10] to avoid absorption in a colder surrounding vapor layer. The fairly broad spectral bandwidth causes an error of less than 2% up to 15,000 K. The inclination of the observed surface should have no influence, from Lambert's law. Also, the optical path of the pyrometer remains unchanged during the experiment. Thus the "only" problem is to determine the intensity at a known temperature and to know the emissivities $\varepsilon(T)$ for the wavelength λ.

Usually, the melting of the wire can be clearly identified in the pyrometer signal. The melting temperature at atmospheric pressure is known, and the emissivity is assumed to be constant for all temperatures above melting [1].

Figure 2 shows a plot of the temperature versus dissipated energy for uncoated tungsten wires for different rates of energy input at melting (lines without symbols). Such curves are also given by other authors (triangle [11]; circle [1]; diamond [20]) or can be calculated from the dissipated energy and a given value of specific heat (squares [12]). Our experiments show the best agreement with the results in Ref. 1 in the solid as well as in the fluid state.

Unfortunately, uncoated tungsten wires can be used only up to 7000 K. Above this temperature the thermal electron emission causes a surface discharge that prevents further measurements. To avoid this, a wire with a coating of 50-μm PTFE is used. This layer "keeps the current in the wire" but inhibits the expansion. Thus, the wire explosion is not carried out anymore at ambient pressure but at a considerably higher pressure depending on the rate of energy input with the effect that the melting temperature rises correspondingly to the melting line. Assuming the specific heat in the solid and in the liquid to be independent from the pressure, the temperature curves were fitted to the data from [1] by varying the melting

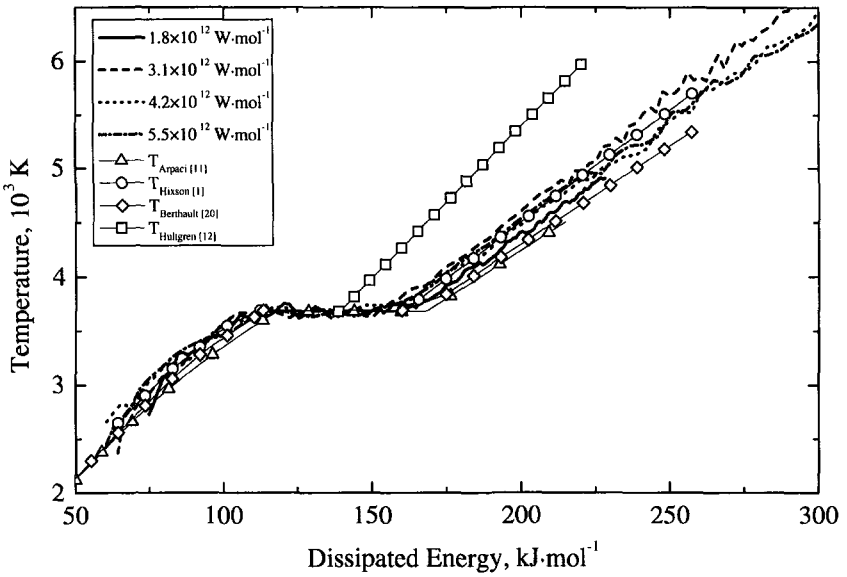

Fig. 2. Temperature as a function of energy for pure tungsten wires. Lines, experiments with different rates of energy input. Values from Ref. 1, circles; Ref. 11, triangles; Ref. 12, squares; Ref. 20, diamonds.

temperature, which is used to calibrate the pyrometer. The rise in the melting temperature is also reflected in the rise of the resistance at melting.

Figure 3 shows the same measurements as shown in Fig. 2 but for PTFE-coated wires and the corresponding resistance. The melting is noted (thin lines) for the experiment with 3.1×10^{12} W · mol^{-1}, to show the good coincidence. The beginning of melting is better expressed at the temperature which begins to rise before its end, mainly because of the higher pressure inside the wire. Therefore, the end of melting was determined from the resistance [13]. The shift of the melting with increasing rate of energy input can be seen in the resistance curves as well as in the temperature curves. The good agreement between all measured curves (with modified melting temperature) and the one from Ref. 1, which coincides with the measurements at atmospheric pressure, shows the technique yields reliable results.

The heat of fusion of uncoated wires appears to be independent of the rate of energy dissipation and was measured to be $50 \cdot 5 \pm 3$ kJ · mol^{-1}. For coated wires it ranges between 48 and 60 kJ · mol^{-1}. Other authors found values between 46.7 and 61.2 kJ · mol^{-1} [13].

Up to now, the emissivity has been assumed to be constant at temperatures above the melting temperature because of a lack of available

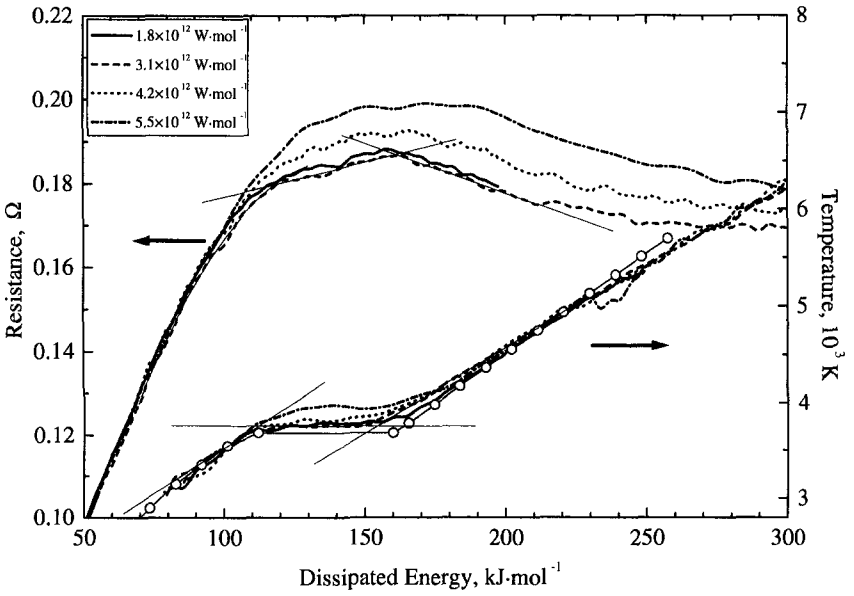

Fig. 3. Temperature and resistance as a function of energy for coated tungsten wires. Lines, experiments with different rates of energy input. Circles, calculated temperature according to Ref. 1. Thin lines, determination of melting for the experiment with 3.1×10^{12} W · mol^{-1}.

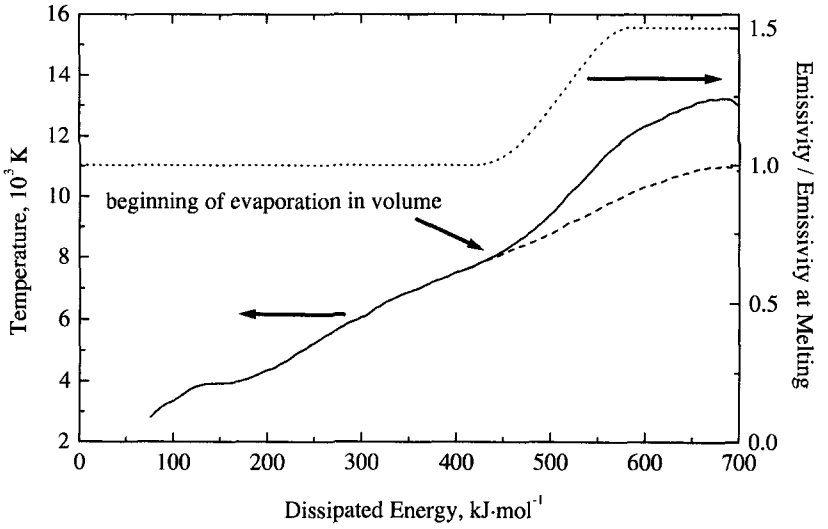

Fig. 4. Temperature and emissivity as a function of energy. Filled line, original temperature; dashed line, corrected temperature; dotted line, emissivity.

data. There is only one hint from a measurement in liquid tungsten up to 3778 K [14], where the emissivity for $\lambda = 680$ nm decreases about 15% compared with the one at melting. This behavior is considered in Ref. 15.

A different situation occurs at temperatures above 8000 K (see Fig. 4). Under the given condition of very rapid heating, vaporization in the volume of an outer shell of the wire takes place [8]. This means, that the observed surface is a two-phase mixture changing from bubbles in liquid to tiny droplets in vapor. Such structure will contain a lot of cavities that may lead to a higher effective emissivity [16].

Figure 4 shows the temperature versus energy for one experiment (4.2×10^{12} W · mol^{-1}). Between 8000 and 9000 K, the slope of the curve rises steeply. This would correspond to a decrease of specific heat by a factor of two. There is no known physical reason for such behavior. A rise in emissivity up to about 150% of the value of the pure liquid, however, would suggest very reasonable temperature behavior.

4. MEASUREMENT OF DENSITY

The density $\rho(t)$ is calculated from the radius $r(t)$ of the wire under the conditions of homogeneity and only radial expansion. The first condition is met according to a model used in Ref. 8. The second is checked by four framing images which are taken during the observation period.

The radius is derived from streak images of the shadow graph of the wire. Therefore, the wire is backlighted with an argon–ion laser at 515 nm and observed through a narrow interference filter. For every instance of time, the distance between the maximum local derivatives of the smoothed intensity is calculated and is taken as the diameter.

In the case of pure tungsten wire, the density can be calculated directly:

$$\rho(t) = \left(\frac{r(t=0)}{r(t)}\right)^2 19.3 \times 10^3 \text{ kg} \cdot \text{m}^{-3} \tag{3}$$

If the wire is surrounded by a coating, a change of radius has to propagate through this layer before it can be seen outside. The radius changes slowly compared with the speed of sound in the coating. Thus, the radius of the wire $r(t)$ is calculated from the measured radius $R(t)$:

$$r(t) = R\left(t + \frac{d(t)}{c_{\text{s, PTFE}}}\right) - d(t) \tag{4}$$

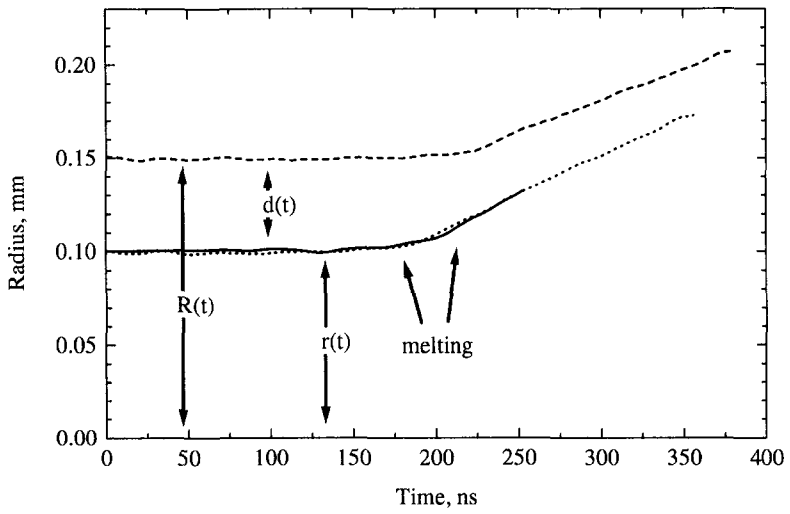

Fig. 5. Radii as a function of time. Dashed line, measured radius $R(t)$ of the coated wire; dotted line, corrected radius $r(t)$ of the metal core; solid line, directly measured radius of a pure wire.

The thickness of the coating $d(t)$ is calculated under the assumptions that it is not heated and its volume remains constant:

$$d(t) = R(t) - \sqrt{R(t)^2 - R(t=0)^2 + r(t=0)^2} \tag{5}$$

The speed of sound of PTFE is given in Ref. 17; $c_{s,\,PTFE} = 1.38\ \text{km} \cdot \text{s}^{-1}$.

Figure 5 shows the measured radius $R(t)$ of a coated wire (dashed curve), the corrected radius $r(t)$ (dotted curve), and the radius of a comparable wire explosion with a pure wire (solid curve). The radii show good agreement. Thus, the density can be determined for temperatures above 7000 K with PTFE-coated wires with a precision of 5% using Eqs. (3) to (5).

5. MELTING CURVE OF TUNGSTEN

The pressure is the most unreliable determined primary thermodynamic value during a wire explosion. The best situation is found for experiments in pressure cells with a defined pressure and a quasi-isobaric run [1–3]. For wire explosions in capillaries [4, 5], a pressure is calculated

from an equation of state, e.g., Ref. 18, the temperature is measured, and the density calculated from an elastic model [5].

For wire explosions in air, the pressure cannot be measured. Even if the temperature and density are known, an equation of state is still unreliable near the vapor pressure curve and, due to the low compressibility, not suitable for pressure determinations.

For melting, a pressure may be found from the shift of the melting temperature with the rising rate of energy dissipation. In Refs. 19 and 21 the melting curve is measured experimentally. Using the law of Clausius–Clapeyron and integrating, the melting curve can also be calculated from the difference of the molar volume between solid and liquid at melting $\Delta V_{s,l}$ and the melting entropy ΔS_{melt} or from the heat of fusion ΔH_{melt} and the melting temperature T_{melt}, respectively,

$$\frac{dp}{dT} = \frac{\Delta S_{melt}}{\Delta V_{s,l}} = \frac{\Delta H_{melt}}{T_{melt}\,\Delta V_{s,l}} \tag{6}$$

Table I shows these values from different authors and from our experiments. With the values given in Refs. 1, 3, and 11, a value for dp/dT_{melt} was calculated and then strongly extrapolated. In this work the value was determined for four temperatures. After an interpolation and integration, a melting curve is found up to a pressure of 3.8 GPa and a temperature of 3940 K; see Fig. 6 (filled line). The melting curve of this work agrees remarkably good with the directly measured curves from Refs. 19 and 21 (dashed lines with circles and squares). The crosses mark the temperatures at which experimental values were used.

Table I. Derivative of the Melting Curve from the Literature and the Experiment

Ref./experiment	T_{melt} (K)	ΔH_{melt} ($kJ \cdot mol^{-1}$)	ΔV ($cm \cdot mol^{-1}$)	dp/dT_{melt} ($MPa \cdot K^{-1}$)
Hixson and Winkler [1] (0.3 GPa)	3690	47.8	0.286	45.3
Kaschnitz et al. [3]	3680	47.1	0.434	29.5
Arpaci and Frohberg [11] (atmospheric pressure)	3683	50.0	0.484	28.2
Hultgren et al. [12] (up to 5 GPa)	$T_{melt}(p)$	Directly	Measured	13.4
Musella et al. [21] (up to 0.2 GPa)	$T_{melt}(p)$	Directly	Measured	11.2
1.8×10^{12} W · mol^{-1}	3730	48.3	0.859	15.1
3.1×10^{12} W · mol^{-1}	3760	48.9	1.012	12.9
4.2×10^{12} W · mol^{-1}	3820	56.4	1.259	11.7
5.5×10^{12} W · mol^{-1}	3950	59.7	0.819	18.4

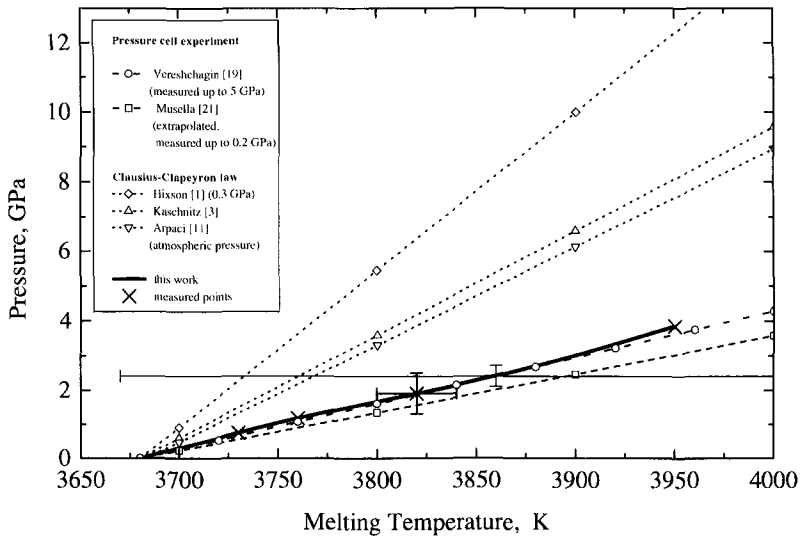

Fig. 6. Melting curves of tungsten. Dashed lines—experiments: Ref. 19, circles and error bars at 3860 K; Ref. 21, squares. Dotted lines—calculations with Causius–Clapeyron law with values from Ref. 1, diamonds; Ref. 3, up triangles; Ref. 11, down triangles. This work: thick line with crosses for measured points and error bars at 3820 K.

6. CONCLUSION

The melting temperature of tungsten was measured for different rates of energy dissipation during a submicrosecond wire explosion with coated and uncoated wires. For coated wires the melting temperature rises with increasing rate of energy dissipation. This may be explained with a higher pressure due to the inertia of the coating. With the help of the Clausius–Clapeyron law and values for the melting energy, the melting temperature, and the change in molar volume during melting from the experiment, a preliminary melting curve was derived, which agrees well with directly measured curves from the literature, which recommends fast-wire explosion experiments also for the determination of melting curves.

REFERENCES

1. R. S. Hixson and M. A. Winkler, *Int. J. Thermophys.* **11**:709 (1990).
2. U. Seydel and W. Kitzel, *J. Phys. F Metal Phys.* **9**:L153 (1979).
3. E. Kaschnitz, G. Pottlacher, and L. Windholz, *High Press. Res.* **4**:588 (1990).
4. A. I. Savvatimski, *Int. J. Thermophys.* **17**:495 (1996).
5. A. W. Desilva and H. J. Kunze, *Phys. Rev. E* **49**:4448 (1994); I. Krisch, Ph.D. thesis (University of Bochum, Germany, 1997).

6. H. Hess, *Phys. Chem. Liq.* **30**:251 (1995).
7. A. Kloss, T. Motzke, R. Grossjohann, and H. Hess, *Phys. Rev. E* **54**:5851 (1996).
8. A. Kloss, A. D. Rakhel, and H. Hess, *Int. J. Thermophys.* **19**:983(1998).
9. Goodfellow No. W005148 and Advent No. W558711.
10. NIST Standard Reference Database 38, NIST Spectroscopic Properties of Atoms and Atomic Ions Database (NIST, Gaithersburg, MD).
11. E. Arpaci and M. G. Frohberg, *Z. Metallkd.* **75**:614 (1984).
12. R. Hultgren, P. D. Desai, D. T. Hawkins, M. Gleiser, K. K. Kelley, and D. D. Wagman, *Selected Values of the Thermodynamic Properties of the Elements* (American Society for Metals, Metals Park, OH, 1972).
13. J. L. McClure and A. Cezairliyan, *Int. J. Thermophys.* **14**:449 (1993).
14. J.-P. Hiernault, R. Beuker, M. Hoch, T. Matsui, and R. W. Ohse, *High Temp.-High Press.* **18**:627 (1986).
15. H. Hess, A. Kloss, and H. Schneidenbach, *Int. J. Thermophys.* **20**:1281 (1999).
16. R. E. Bedford, in *Radiation Thermometry*, D. P. DeWitt and G. D. Nutter, eds. (Wiley-Interscience, New York, 1988).
17. *Encyclopedia for Polymer Science*, 2nd ed. (1989), Vol. 1, p. 147.
18. SESAME Library, T-1, MS-B221 (Los Alamos National Laboratory, Los Alamos, NM).
19. L. F. Vereshchagin and N. S. Fateeva, *JETP* **28**:797 (1969); D. A. Young, *Phase Diagrams of the Elements* (University of California Press, Berkeley, Los Angeles, Oxford, 1991), p. 175.
20. A. Berthault, L. Arles, and J. Matricon, *Int. J. Thermophys.* **7**:167 (1986).
21. M. Musella, C. Ronchi, and M. Sheindlin, *Int. J. Thermophys.* **20**:1177 (1999).